Electron Diffraction by Gases

L. R. Maxwell, S. B. Hendricks, and V. M. Mosley

Citation: The Journal of Chemical Physics **3**, 699 (1935); doi: 10.1063/1.1749580
View online: http://dx.doi.org/10.1063/1.1749580
View Table of Contents: http://scitation.aip.org/content/aip/journal/jcp/3/11?ver=pdfcov
Published by the AIP Publishing

Electron Diffraction by Gases

L. R. MAXWELL, S. B. HENDRICKS AND V. M. MOSLEY, *Bureau of Chemistry and Soils, Washington, D. C.*

(Received August 25, 1925)

The method of electron diffraction is used for determining the C−O−C valence angle (α) in 4,4′ diiododiphenyl ether $[(C_6H_4I)_2O]$ and the molecular structures of phosphorus (P_4) and arsenic (As_4). The electron diffraction photographs were analyzed by four different methods as follows: (1) Visual measurements, (2) measurements of densitometer records, (3) conversion of densitometer records into relative intensity curves, (4) comparison of transformed intensity curves obtained by multiplying the intensity of scattering by $[(1/\lambda)\sin\theta/2]^2$ which produces prominent maxima for measurement. The valence angle α was found to be $118\pm3°$ for 4,4′ diiododiphenyl ether, definitely greater than the oxygen valence angle found for simpler types of molecules. Phosphorus and arsenic molecules were found to have a regular tetrahedral structure within the limits of experimental error, the atomic separations being 2.21A and 2.44A, respectively, [methods (1) and (2) were used for the case of arsenic]. The minimum atomic distances as found by crystal structure analysis for phosphorus and arsenic are approximately the same as the atomic separations obtained for the gas molecules, showing in addition that these distances do not change greatly when the bond angle decreases from 100° to 60°.

VALENCE ANGLE OF OXYGEN IN 4,4′ DIIODODIPHENYL ETHER

IT IS a matter of considerable theoretical importance to ascertain the value and the possible constancy of the valence angle of oxygen. This can be accomplished directly by electron diffraction methods and has already been carried out for several molecules.[1] The compound 4,4′ diiododiphenyl ether is unusually well adapted for this purpose on account of the predominant scattering of electrons by the iodine atoms. As a first approximation it can be considered as a triatomic molecule I−O−I, with an I−O distance of 6.26A.[2] The geometry of the complete molecule can, with considerable confidence, be taken as that shown in Fig. 1 which has two perpendicular planes of symmetry. Deviation from this model by rotation about the C−O bond would bring the carbon atoms of separate benzene rings into juxtaposition for values of α less than 150°. Actually the analysis is not sensitive even to this alternative since rotation of the groups would not materially change the intensity expressions. The theoretical intensity of electron scattering for the model assumed in Fig. 1 can be expressed as follows:

$$I(x_{cc}) = I_{II} + I_{IC} + I'_{IC} + I_{IO} + I_{CO} + I_{CC} + I_{inc},$$

where

$$I_{II} = 2\psi_I^2(1+(\sin px_{cc})/px_{cc}) \quad \text{coherent scattering between iodine atoms}$$

$$I_{IC} = 4\psi_O\psi_I\left(\frac{\sin 1.48x_{cc}}{1.48x_{cc}} + 2\frac{\sin 2.14x_{cc}}{2.14x_{cc}} + 2\frac{\sin 3.1x_{cc}}{3.1x_{cc}} + 2\frac{\sin 3.48x_{cc}}{3.48x_{cc}}\right) \quad \text{iodine to carbon cross product terms, independent of valence angle}$$

$$I'_{IC} = 4\psi_O\psi_I\left(\frac{\sin qx_{cc}}{qx_{cc}} + 2\frac{\sin rx_{cc}}{rx_{cc}} + 2\frac{\sin sx_{cc}}{sx_{cc}} + \frac{\sin tx_{cc}}{tx_{cc}}\right) \quad \text{iodine to carbon cross product terms dependent on valence angle}$$

$$I_{IO} = 4\psi_O\psi_I\left(\frac{\sin 4.41x_{cc}}{4.41x_{cc}}\right) \quad \text{iodine to oxygen scattering } \psi_O \text{ replaced by } \psi_C$$

$$I_{CO} = 4\psi_O\psi_C\left(\frac{\sin x_{cc}}{x_{cc}} + 2\sin\frac{3^{\frac{1}{2}}x_{cc}}{3^{\frac{1}{2}}x_{cc}} + 2\frac{\sin 2.64x_{cc}}{2.64x_{cc}} + \frac{\sin 3x_{cc}}{3x_{cc}}\right) \quad \text{carbon to oxygen cross product terms independent of valence angle; } \psi_O \text{ is replaced by } \psi_C$$

[1] L. E. Sutton and L. O. Brockway, J. Am. Chem. Soc. **57**, 473 (1935); H. Boersch, Monat. f. Chemie **65**, 311 (1935).

[2] This value can be obtained from the I−C distance 2.00A as found by electron diffraction results from para diiodobenzene (see reference 4), the known C−C distances in the benzene molecule and from the assumed C−O separation of 1.42 (theoretical value for the single bond C−O separation).

$$I_{CC}=12\psi_C\psi_C\left(1+\frac{2\sin x_{cc}}{x_{cc}}+\frac{\sin 2x_{cc}}{2x_{cc}}+\frac{2\sin 3^{\frac{1}{2}}x_{cc}}{3^{\frac{1}{2}}x_{cc}}\right)$$ ..... total coherent scattering from two independent benzene rings with cross product terms between them omitted

$$I_{inc}=\frac{1}{\left(\frac{\sin\theta/2}{\lambda}\right)^4}[106\,S(\nu_I)+72S(\nu_C)+8S(\nu_O)]$$ ..... incoherent scattering from all the atoms in the molecule (hydrogen atoms omitted)

where

$$x_{cc}=4\pi l_{cc}\left(\frac{\sin\theta/2}{\lambda}\right), \qquad l_{cc}=\text{C}-\text{C distance}=1.42\text{A}$$

$$\psi_i=(Z_i-F_i)\Big/\left(\frac{\sin\theta/2}{\lambda}\right)^2, \qquad \nu_i=4\pi b_i\frac{(\sin\theta/2)}{\lambda}$$

Z_i = atomic number, $\qquad b_i=0.176/Z_i^{\frac{1}{2}}$

F_i = atomic scattering factor.*

Electron scattering from the hydrogen atoms has been omitted as also has the C−C scattering between atoms of different benzene rings. Although the relatively large value of ψ_I causes the I_{II} term to be the most important, the other terms considered cannot be omitted since they give an intensity that has pronounced maxima and minima. Results of calculations for various valence angles, C−O−C, are shown in Fig. 2.

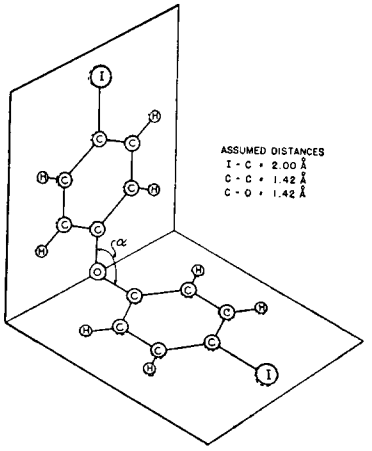

FIG. 1. Diagram of molecular model of 4,4′ diiododiphenyl ether.

* Obtained from calculated values of R. W. James and G. W. Brindley, Phil. Mag. 12, 81 (1931).

TABLE I. *Data on parameters used in calculating electron scattering from 4,4′ diiododiphenyl ether.*

OXYGEN VALENCE ANGLE	p	q	r	s	t
180°	8.82	5.41	5.96	6.96	7.40
120°	7.63	4.99	5.32	6.05	6.45
110°	7.22	4.85	5.11	5.75	6.12
90°	6.24	4.51	4.58	5.06	5.33

Data on the parameters used in these calculations are given in Table I. These curves show only prominences or points of inflection. However, if $I(x_{cc})((\sin\theta/2)/\lambda)^2$ is plotted with respect to x_{cc} or x_{II}, as in Figs. 3 and 4, these prominences are accentuated in such a manner as to give actual maxima that permit unambiguous comparison with the experimental data. Positions of the maxima of the curves shown in Fig. 4 are listed in Table II.

The above calculations are to be compared with the experimental results[3] obtained. Four methods, as given below, have been used in making this comparison. The apparatus used has been described elsewhere.[4]

(1) *Visual measurements.* The photographs were characterized by one very prominent ring appearing at $(1/\lambda)\sin\theta/2=0.24$ with two inner rings that were considerably weaker but easily

[3] We are indebted to Professor R. Q. Brewster of the University of Kansas for a liberal supply of the 4,4′ diiododiphenyl ether which was used in this work.

[4] S. B. Hendricks, *et. al.*, J. Chem. Phys. 1, 549 (1933).

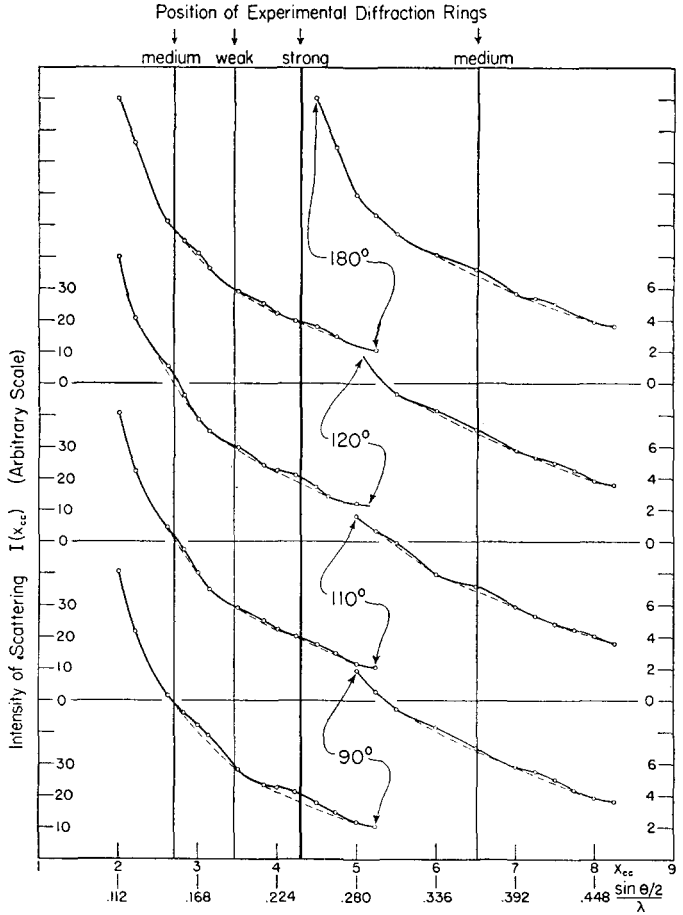

FIG. 2. Theoretical electron scattering curves $I(x_{cc})$ for 4,4′ diiododiphenyl ether. Position of experimental diffraction rings as measured visually are indicated for comparison. The circles represent points calculated in this instance and also for subsequent curves. (Figs. 3, 4, 7, 8, and 9.)

detectable on several photographs. Positions of apparent diffraction maxima as visually measured are shown on Fig. 1 and are listed in Table III. Although this method is possibly open to a psychological error occasioned by the rapidly varying background[5] it is sufficiently accurate to indicate that the valence angle, C−O−C, is probably in the region about 110° or 120°.

(2) *Densitometer measurements.* Results obtained from densitometer records are recorded in Table IV and are illustrated by the typical record shown in Fig. 5a. The position of the single prominent ring, the third maxima of Table IV, is determined by first constructing as a base line a smooth continuation of the densitometer curve through the region in which the prominence occurs and then bisecting the area between these two curves by a vertical line. A similar method is applied to the theoretical intensity curve and values so obtained are also listed in Table IV. These data are useful in

[5] For the discussion of the possible psychological errors arising in locating visually the position of electron diffraction rings see, for instance, Linus Pauling and L. O. Brockway, J. Chem. Phys. 2, 867 (1934).

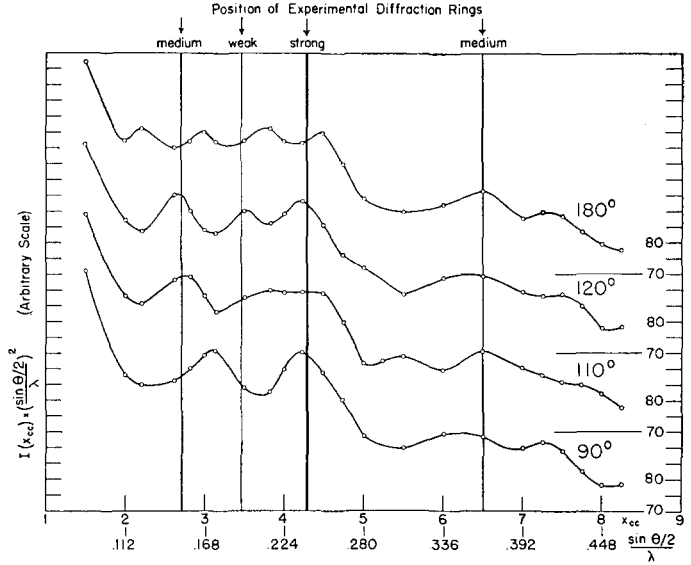

FIG. 3. Theoretical electron scattering curves $I(x_{cc})[(\sin\theta/2)/\lambda]^2$ for 4,4′ diiododiphenyl ether. Position of experimental diffraction rings as measured visually are indicated for comparison.

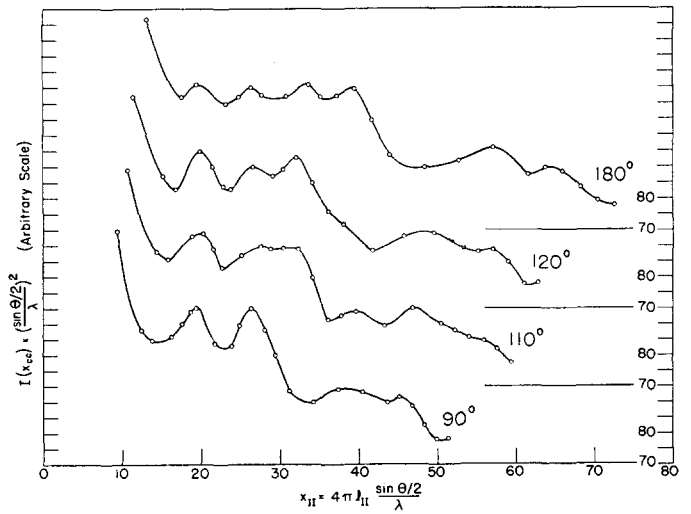

FIG. 4. Theoretical electron scattering curves $I(x_{cc})[(\sin\theta/2)/\lambda]^2$ for 4,4′ diiododiphenyl ether with respect to $x_{II}=4\pi l_{II}[(\sin\theta/2)/\lambda]$ made to illustrate how closely the scattering can be represented by a pure diatomic iodine structure.

TABLE II. *A summary of the position of calculated interference maxima for 4,4′ diiododiphenyl ether expressed in terms of* $x_{II}=4\pi l_{II}(1/\lambda)\ \sin\theta/2$.

Valence angle	1st maximum C	1st maximum D	2nd maximum C	2nd maximum D	3rd maximum C	3rd maximum D	4th maximum C	4th maximum D
90°	19.6	19.50	27.0	26.5	38.9	38.4	46.30	45.2
110°	20.3	19.8	27.4	27.6	33.2	shoul-der	40.2	39.7
120°	20.4	20.0	27.1	26.8	32.7	32.2	49.0	48.2
180°	—	19.5	26.5	26.4	33.4	33.2	39.9	39.0
For pure I-I scattering maxima would come at approximately	20.37		26.66		32.9		39.2	

C Position of humps located by using complete intensity formula $I(x_{cc})$ including incoherent scattering (method of bisecting areas used).
D Position of maxima located from $I(x_{cc})\times((\sin\theta/2)/\lambda)^2$ curves, real maxima measured in all cases.

TABLE IV. *Results of densitometer measurements on the electron diffraction photographs of 4,4′ diiododiphenyl ether and comparison with theory.*

Plate No.	λ	Position of humps measured by bisecting areas, expressed in units of $(1/\lambda)\sin\theta/2$ 1st maximum	2nd maximum	3rd maximum
12	0.0770	absent	absent	0.242
13	.0826	absent	absent	.244
14	.0838	absent	absent	.246
15	.0863	absent	absent	.246
Average				0.244 ±.002
Expressed in units of x_{cc}				4.35 ±.004
Theoretical position of corresponding prominence expressed in units of x_{cc}			90°	4.33
			110°	4.60
			120°	4.29
			180°	4.55

differentiating between "α" (Fig. 1) equal to 110° and 120° since the 90° and 180° cases are eliminated by the visual measurements. The experimental value, $x_{cc}=4.35$, is in good agreement with the theoretical value, 4.28, for $\alpha=120°$, and in definite disagreement with the 110° model whose $x_{cc}=4.60$.

(3) *Relative intensity measurements.* Since the above method involved the questionable comparison of an intensity curve with a densitometer record it was considered feasible to obtain experimental values for the relative intensity of scattering. This required the determination of the relationship between the photographic density and the intensity of the electrons, which was obtained by means of plate calibrations.[6] Fig. 5b shows a relative intensity distribution obtained in this manner from the densitometer record shown in Fig. 5a. The method of bisecting areas as described above was applied to this curve and leads to a value of $x_{cc}=4.35$ for the prominent ring, which is the same as that obtained from the densitometer records. This corresponds to $\alpha=120°$.

(4) $I(\theta)\times[(1/\lambda)\ \sin\theta/2]^2$. It has been shown above that it is possible to obtain theoretical curves with true maxima by multiplying the intensity of scattering $I(x_{cc})$ by $[(1/\lambda)\sin\theta/2]^2$. We can obtain equivalent experimental curves

TABLE III. *Visual measurements on the electron diffraction photographs of 4,4′ diiododiphenyl ether* (position of maxima)

Plate No.		1st maximum sin θ/2 / λ	1st maximum description	2nd maximum sin θ/2 / λ	2nd maximum description	3rd maximum sin θ/2 / λ	3rd maximum description	4th maximum sin θ/2 / λ	4th maximum description
1	0.0577					0.232	strong	present	
2	.0598					.239	strong	0.368	
3	.0650					.249	strong	present	
4	.0662					.238	strong	present	
5	.0662	0.152	medium	0.187	weak	.238	strong		
6	.0662	.152	medium	.194	weak	.238	strong		
7	.0680	.153	medium	.194	weak	.239	strong		
8	.0686	.150	medium	.195	very weak	.251	strong	.362	
9	.0700					.238	strong		
10	.0700					.232	strong		
11	.0765	.153	weak	.200	weak	.249	strong	.368	
12	.0780					.235	strong		
13	.0830					.247	strong		
14	.0838					.238	strong		
15	.0863	present	weak			.242	strong		
Average value		0.152 ±.006		0.194 ±.01		0.240 ±.005		0.366	
Expressed in units of x_{cc}		2.71±.107		3.46±.18		4.29±.089		6.53	

[6] Plate calibrations were made for the type of emulsion used (Eastman lantern slide slow emulsion) by exposing different portions of the calibration plate to the electron beam for different times of exposure. Since the reciprocity law is known to hold accurately at these voltages (A. Becker and E. Kipphan, Ann. d. Physik **10**, 15 (1931)) the calibrations could be obtained. Separate plates were used for the calibration. They were developed with the electron diffraction plates so that both received exactly the same development.

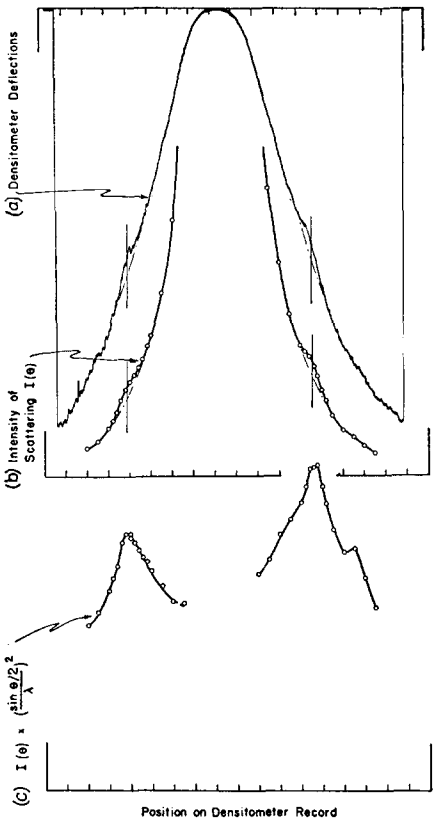

FIG. 5. (a) Densitometer record of the prominent interference ring of 4,4′ diiododiphenyl ether at approx. $(1/\lambda)\sin\theta/2=0.24$. (b) Experimental relative intensity curve made from (a) after plate calibrations. Vertical line through hump shows how area under curve is bisected. (c) Transformed electron scattering curve constructed from (b) in order to produce real maxima for measurement.

by the same method, as illustrated for the molecule 4,4′ diiododiphenyl ether in Fig. 5c.[9] This results in the production of a maximum at $x_{ee}=4.32$ which is in approximate agreement with the corresponding theoretical value of 4.20 for $\alpha=120°$ and again eliminates the model with $\alpha=110°$ since in that case only a broad maxima is obtained.

A less exact theoretical treatment has been used by Wierl[7] and later workers[8] who have compared their experimental results with calculated electron scattering curves in which ψ_i is replaced by Z_i and the incoherent scattering is omitted. This was done in order to simplify the calculation and also to produce true maxima in the calculated curves. While it is apparently satisfactory, particularly for large values of $(1/\lambda)\sin\theta/2$, it must be used in all instances with considerable caution. The approximate treatment does not give the true relative intensity of scattering. In many cases considerable additional information can be obtained if the correct theoretical intensity of scattering is known.

An alternative method for determining the valence angle

More direct advantage can be taken of the predominance of the I_{II} scattering term than is apparent in the above analysis. In doing this it is most convenient to consider x_{II} as the variable so that maxima given by I_{II} will not be a function of α. From Fig. 4 and Table II it can be seen that the position of the first prominence is approximately independent of α and closer analysis shows that this must be caused by the prominent I_{II} term. Given the geometry of

TABLE V. *Determination of the I–I separation and valence angle of oxygen in 4,4′ diiododiphenyl ether.*

	1ST MAXIMUM		2ND MAXIMUM		3RD MAXIMUM	
METHOD OF MEASUREMENT	$\frac{\sin\theta/2}{\lambda}$	I_{II}(A) for $x_{II}=20.4$	$\frac{\sin\theta/2}{\lambda}$	I_{II}(A) for $x_{II}=27.1$	$\frac{\sin\theta/2}{\lambda}$	I_{II}(A)
Visual	0.152±0.006 (5)	10.68±0.40	0.194±0.01 (5)	11.12±0.50	0.240±0.005 (15)	10.84±0.20 for $x_{II}=32.7$
b.a. dens. rec'd					0.244±.002 (4)	10.66± .09 for $x_{II}=32.7$
b.a. rel. int. curve					0.242 (1)	10.75 for $x_{II}=32.7$
$I(\theta)\times((\sin\theta/2)/\lambda)^2$					0.242 (1)	10.59 for $x_{II}=32.2$

b.a. means bisecting area.
Number in parentheses represents number of measurements made. Most probable I−I distance, 10.75±0.20A. Most probable valence angle, 118±3°.

[7] R. Wierl, Ann. d. Physik **13**, 453 (1932).
[8] See references listed by Louis R. Maxwell, *et al.*, J. Chem. Phys. **2**, 331 (1934).
[9] A feature of this treatment lies in the fact that it does not require the accurate location of the origin of the angle of scattering on the densitometer record but instead it

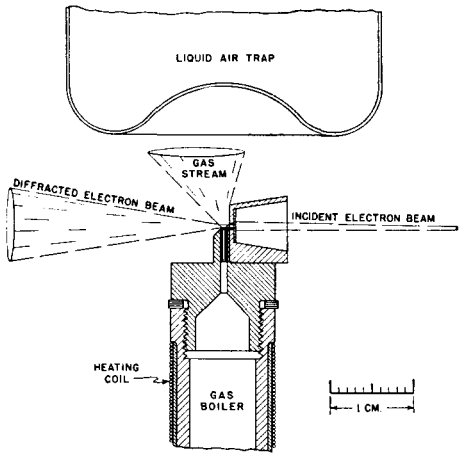

FIG. 6. Improved form of gas boiler containing the electron diaphragm as an integral unit.

Fig. 1 this leads to 118° as the value of α corresponding to an I−I distance of 10.70A. With this approximate limitation of α the method is also found to be applicable to the second and to the more accurately measured third prominence. Combination of these results, as shown in Table V, lead to a valence angle, C−O−C, of $118\pm3°$.

Discussion

The analysis of the rotation vibration spectrum of the water molecule by Mecke and coworkers[10] leads to 104°–106° as the valence angle of oxygen. This angle has been determined in several other compounds from analysis of electron diffraction patterns. Thus Sutton and Brockway[11] found $105\pm5°$, $111\pm2°$, and $111\pm4°$ for the oxygen valence angle in F_2O, Cl_2O, and $(CH_3)_2O$, respectively, while Boersch[12] found $\alpha=100\pm3°$ in F_2O. These values are all definitely lower than that found above for 4,4′ diiododiphenyl ether.

It is also possible to calculate the valence angle of oxygen from measurements of electric moments although such a method involves several questionable assumptions. This method has been applied to 4,4′ dibromodiphenyl ether, 4,4′ dibromobenzene, and diphenyl ether, by Hampson, Farmer, and Sutton.[13] They found $\alpha=142°$ but a similar analysis by Pai[14] gave a value of 126.9°. More recently Sutton and Hampson* have revised their value of α to $128\pm4°$ which is closer to the electron diffraction results. Hare and Mack[15] obtain $\alpha=107°$ from viscosity determinations of diphenyl ether by the use of shadow areas obtained from various molecular models. This procedure does not possess the accuracy of electron diffraction methods so therefore it can be considered only as substantiating the electron diffraction value of 118°.

MOLECULAR STRUCTURE OF PHOSPHORUS AND ARSENIC

These two elements are of particular interest in that they form homonuclear molecules of high symmetry in the vapor phase and extended homopolar nets in some of their crystalline forms. The opportunity is thus present for comparing the internuclear separations and valence angles occurring in these different forms. Vapor density measurements indicate that the molecules are predominantly tetratomic under the experimental conditions described below.

In order to obtain the requisite vapor pressures it was necessary to heat phosphorus to about 200°C and arsenic to *ca.* 500°C. This was conveniently accomplished in a boiler of the type shown in Fig. 6. A diaphragm for restricting the electron beam was attached to the boiler in such a manner as to insure electron collisions with the molecular beam issuing from the boiler. The entire unit was maintained at a sufficiently high temperature to prevent any condensation of the scattering substance on the electron diaphragm. The cross section of the electron beam incident on the diaphragm was large enough to accommodate any expansion or displacement of the boiler unit. Each substance required a some-

can be shown that an arbitrary origin differing as much as 10 percent in position from the true origin can be used for obtaining the position of the experimental maxima without introducing any detectable error.

[10] See for instance H. A. Stuart, *Molekulstruktur*, p. 313 (1934).

[11] Reference 1.

[12] Reference 1.

[13] G. C. Hampson, R. H. Farmer and L. E. Sutton, Proc. Roy. Soc. **A143**, 147 (1934). See also Stuart's *Molekulstruktur*, p. 142.

[14] N. Gopala Pai, Ind. J. Phys. **9**, 121 (1934).

* L. E. Sutton and G. C. Hampson, Trans. Faraday Soc. **31**, 945 (1935).

[15] Weston A. Hare and Edward Mack, Jr., J. Am. Chem. Soc. **54**, 4272 (1932).

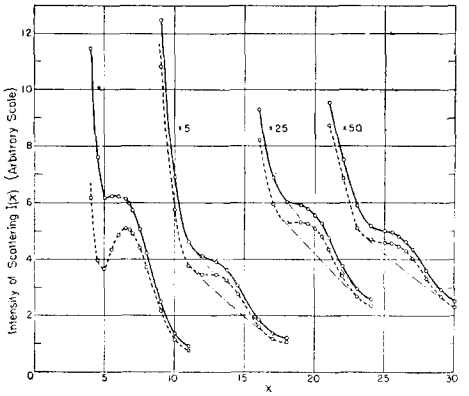

FIG. 7. Theoretical electron scattering curves of phosphorus (P_4) for a regular tetrahedral model. The dotted curve represents the coherent scattering while the full curve gives the total intensity (incoherent and coherent).

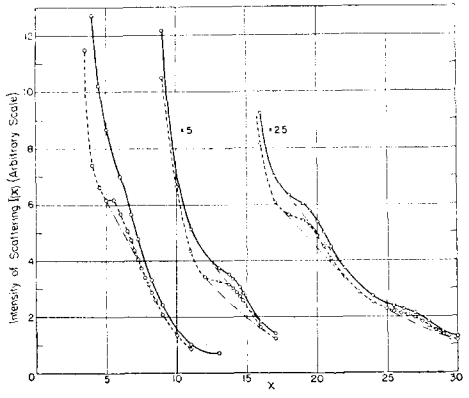

FIG. 8. Calculations for P_4 similar to Fig. 7 except for a square model.

what special technique owing to the fire hazard from phosphorus and the readiness with which arsenic alloys with hot metals. Carefully purified phosphorus was distilled in an inert atmosphere into a glass cup and then covered with a small amount of water. This cup was then introduced into the furnace shown in Fig. 6 and the water evaporated. Fire hazards were eliminated by condensing CCl_4 vapor on the exposed phosphorus surfaces at the end of the exposures. Arsenic was purified from the oxide by heating, in nitrogen, to about 600°C. It then was introduced into a quartz furnace similar to the metal one shown in Fig. 6. Electron diffraction photographs from phosphorus were taken with plate distances of 26.2 cm and 10 cm while only the shorter distance was used for arsenic.

Complete electron scattering curves for phosphorus are shown for a regular tetrahedral model in Fig. 7 and for a square model in Fig. 8. $I(x)\times((\sin\theta/2)/\lambda)^2$ is plotted as a function of x for these two cases in Fig. 9.[16] The intensity equations used in calculating these curves are for a regular tetrahedron:

$$I(x)\dagger = 4\psi_p^2\left(1+3\frac{\sin x}{x}\right)+I_{inc}$$

and for a square array:

$$I(x)=4\psi_p^2\left(1+2\frac{\sin x}{x}+\frac{\sin\sqrt{2}x}{\sqrt{2}x}\right)+I_{inc},$$

where

$$\psi_p=\frac{Z_p-F_p}{\left(\frac{\sin\theta/2}{\lambda}\right)^2},\qquad I_{inc}=\frac{60\times S(\nu_p)}{\left(\frac{\sin\theta/2}{\lambda}\right)^4},$$

$$x=4\pi l_{p-p}\frac{\sin\theta/2}{\lambda},\qquad l_{p-p}=\text{P}-\text{P separation}.$$

Positions of theoretical interference maxima for the two models as obtained by the approximate and rigorous methods of calculations are listed in Table VI. The approximate methods lead to important differences particularly in the case of the first maximum.[17] This maximum shows the greatest variance for the two models being prominent in the tetrahedral case and almost absent for the square model (compare Figs. 7 and 8). These calculations also can be used for the arsenic molecule without introducing any appreciable error since the only difference between the two cases arises in the magnitude of the ψ factors and the incoherent scattering. These changes would not materially alter the position of the outer prominences.

[16] It is necessary to assume at least an approximate value of $l_{P-P}=2.30$A in order to obtain the ψ functions. Although this value was also used here for obtaining the $I(x)\times((\sin\theta/2)/\lambda)^2$ functions it was not required because it can be shown that the position of these theoretical maxima are independent of l_{P-P}, in fact the expression $I(x)\times x^2$ could be used for locating the maxima.

† In these equations and the foregoing the constant factor is omitted.

[17] The value of intensity relationships has been previously described (Louis R. Maxwell, *et al.*, reference 8).

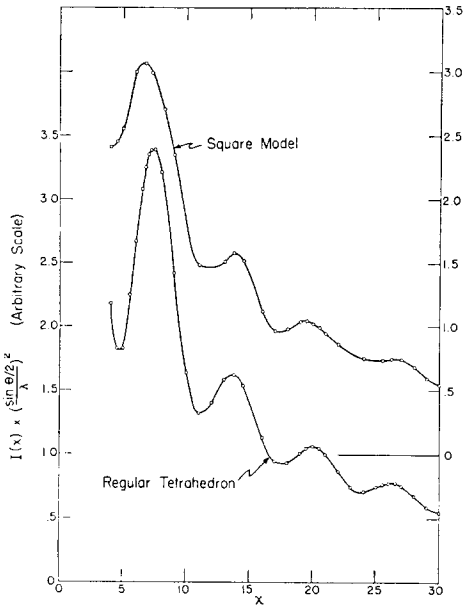

FIG. 9. Transformed theoretical electron scattering curves for P_4 obtained from the total scattering curves shown in Fig. 7 and Fig. 8.

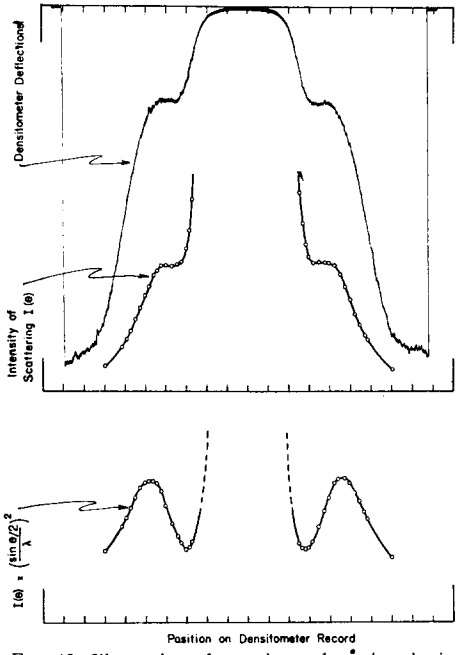

FIG. 10. Illustration of experimental results obtained for the first maximum of P_4. Method of treatment same as described in Fig. 5.

TABLE VI. *Theoretical positions of interference maxima for phosphorus.*

	1ST MAXIMUM				2ND MAXIMUM				3RD MAXIMUM				4TH MAXIMUM			
MODEL	*A*	*B*	*C*	*D*	*A*	*B*	*C*	*D*	*A*	*B*	*C*	*D*	*A*	*B*	*C*	*D*
Regular Tetrahedron	7.72	6.50	6.00	7.3	14.06	13.9	13.9	13.6	20.37	20.2	20.2	20.0	26.66	26.5	26.5	26.3
Plane Square	7.75	shoulder	very slight hump	6.6	14.25	14.20	14.30	13.80	19.80	19.80	19.8	19.5	27.0	27.1	27.1	26.6

A. Position of maxima located by using approximate solution in which ψ_i are replaced by Z_i (real maxima measured).
B. Position of maxima located by using complete intensity formula without incoherent scattering (method of bisecting areas used except for first maxima where a real maximum was observed).
C. Position for maxima located by using complete intensity formula incoherent scattering included (method of bisecting areas used except for first maxima where a real maximum was observed).
D. Position of maxima located from $I(x) \times((\sin\theta/2)/\lambda)^2$ curves, real maxima measured in all cases.

TABLE VII. *Average values obtained for* $(1/\lambda)\sin\theta/2$ *from (A) visual and (B) densitometer measurements of electron diffraction photographs of phosphorus* (P_4).

	$(1/\lambda)\sin\theta/2$									
	2ND MAXIMUM		3RD MAXIMUM		4TH MAXIMUM		5TH MAXIMUM		6TH MAXIMUM	
	A	*B*	*A*	*B*	*A*	*B*	*A*	*B*	*A*	*B*
Wave-length range										
0.055 to 0.077A	0.494±0.011	0.497±0.003	0.732±0.007	0.725±0.004	0.954±0.008		1.188±0.005		1.412±0.002	
*	(13)	(4)	(16)	(2)	(9)		(4)		(2)	
l_{P-P}(A) for regular tetrahedron	2.24		2.20		2.21		2.21		2.21	
	(x=13.9)		(x=20.2)		(x=26.5)		(x=32.95)		(x=39.24)	
l_{P-P}(A) for square model	2.30		2.15		2 26		2.19		2.24	
	(x=14.3)		(x=19.8)		(x=27.1)		(x=32.75)		(x=39.7)	

* No. of measurements made given by number in parentheses.

TABLE VIII. *Summary of measurements of the P–P distance (A) in phosphorus (P_4).*

METHOD OF OBSERVATION	1ST MAXIMUM	2ND MAXIMUM	3RD MAXIMUM	4TH MAXIMUM	5TH MAXIMUM	6TH MAXIMUM
Visual		2.24 (13)	2.20 (16)	2.21 (9)	2.21 (4)	2.21 (2)
*b. a. dens. rec'd		2.22 (4)	2.22 (2)			
*b. a. rel. int. curve $I(\theta)$		2.21 (1)				
$I(\theta)\times\left(\frac{\sin\theta/2}{\lambda}\right)^2$	2.25 (1)	2.21 (1)				

No. of measurements made given by number in parentheses.
Most probable structure—regular tetrahedron with P–P distance of 2.21±0.02A.
* b. a. means bisecting area.

TABLE IX. *Experimental results obtained from the electron diffraction photographs of arsenic (As_4).*

	2ND MAXIMUM	3RD MAXIMUM	4TH MAXIMUM	5TH MAXIMUM	6TH MAXIMUM
$(1/\lambda)\sin\theta/2$ visual measurements	0.448±0.005 (10)*	0.654±0.005 (9)	0.861±0.003 (7)	1.068±0.007 (4)	1.268 (1)
l_{As-As} regular tetrahedron	2.47 ($x=13.90$)	2.46 ($x=20.20$)	2.45 ($x=26.50$)	2.45 ($x=32.95$)	2.46 ($x=39.24$)
l_{As-As} square model	2.54 ($x=14.30$)	2.41 ($x=19.80$)	2.50 ($x=27.10$)	2.44 ($x=32.75$)	2.49 ($x=39.70$)
$(1/\lambda)\sin\theta/2$ b. a. dens. rec'd	0.455±0.003 (3)	0.663±0.006 (6)	0.871±0.005 (4)		
l_{As-As} regular tetrahedron	2.43 ($x=13.90$)	2.42 ($x=20.20$)	2.42 ($x=26.50$)		

* No. of measurements made given by number in parentheses.
b. a. means bisecting area.
de Broglie wave-length range 0.0586–0.0708A.
Most probable structure regular tetrahedron with As–As distance 2.44±0.03A.

Experimental intensity curves for the first two rings of the electron diffraction pattern of phosphorus are shown in Figs. 10 and 11. The particular record illustrated in Fig. 10 for the first maximum was an average record. Considerable variation in the shape of this maximum was found so that its exact distribution was not obtained. The character of these relative intensity curves should be compared with the theoretical curves given in Figs. 7 and 8. The prominence of the first maximum serves adequately to eliminate the square model. All the details of the pattern are found to be in substantial agreement with the requirements of a regular tetrahedral molecule. A summary of the experimental data is given in Table VII. Measurements of the P–P distance according to the four methods used above for phosphorus are summarized in Table VIII. Visual measurements on the first maximum are omitted since the errors in locating its theoretical and experimental positions are considerable. The combined data show that the molecule has the form of a regular tetrahedron with a P–P distance of 2.21±0.02A.

The electron diffraction pattern of arsenic is very similar to that of phosphorus and in particular the prominence of the first ring is such as again to eliminate the square model. Results of visual and densitometer measurements are listed in Table IX, while in Fig. 12 is shown a reproduction of a typical photograph obtained. The theoretical positions of the maxima calculated for the phosphorus molecule were used here in comparison with the experimental results for arsenic. We conclude from these data that the arsenic molecule is similar to the P_4 molecule in shape, having a regular tetrahedral structure but with a somewhat greater nuclear separation of 2.44±0.03A.

Discussion

Crystal structure information is available for some of the forms of phosphorus and arsenic. In black phosphorus each atom has three nearest neighbors at a distance of 2.18A[18] with bond angles near 102°. Fourier analysis of the diffraction pattern of red phosphorus[18] indicates that the immediate surrounding of a phosphorus atom is similar to that of the black variety, although the experimental value, 2.28A, for the atomic separation is somewhat greater. Black phosphorus contains molecular nets and it is

[18] Ralph Hultgren, N. S. Gingrich and B. E. Warren, J. Chem. Phys. 3, 351 (1935).

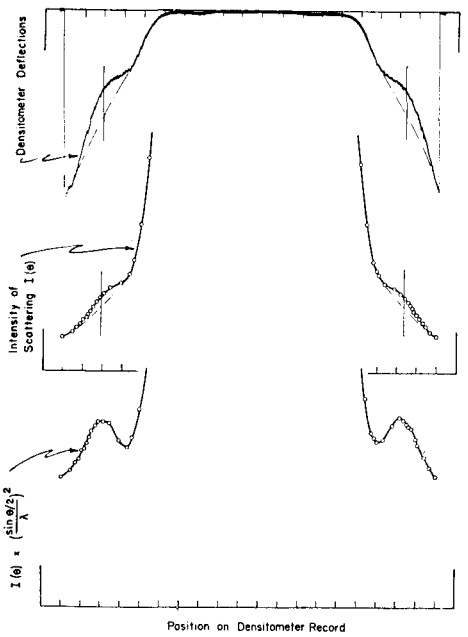

FIG. 11. Illustration of experimental results obtained for the second maximum of P_4. Method of treatment same as described in Fig. 5. Vertical line through prominence shows how area is bisected.

probable that the red modification forms either nets or a spatial array. Crystalline yellow phosphorus on the other hand possibly has a lattice formed from P_4 molecules of the type found in the vapor by the electron diffraction results and on account of their high symmetry they might be expected to be rotating at room temperature.

Arsenic crystallizes into a metallic rhombohedral form and in a supposedly cubic nonmetallic form that can be maintained only in darkness at low temperatures. Crystal structure analysis of the metallic modification[19] indicates that the closest distance of approach of the

[19] A. J. Bradley, Phil. Mag. **47**, 657 (1924); S. V. Olshausen, Zeits f. Krist. **61**, 463 (1935).

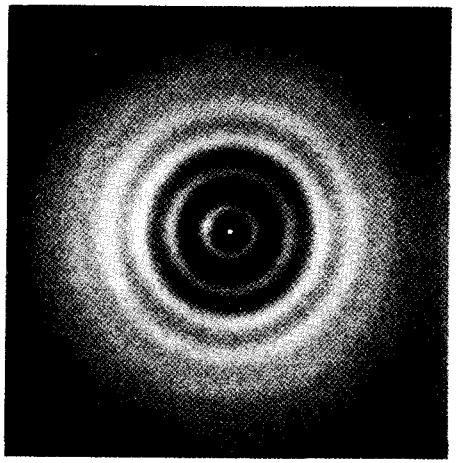

FIG. 12. Reproduction of electron diffraction photograph obtained from arsenic vapor (As_4). de Broglie wavelength 0.0617A, plate distance 10 cm. Magnified 2×.

arsenic atoms is very near to 2.51A and that the bond angles are approximately 97°. The yellow modification is formed when arsenic vapor is condensed at low temperatures. This condition of formation suggests that the lattice consists of As_4 molecules that might be expected to have the configuration found from electron diffraction.

The minimum atomic separations, which are the covalent bond distances, as found by crystal structure analysis for phosphorus and arsenic, are nearly the same as those found in the present work for the gas molecules. This is of particular interest since the bond angle for the tetrahedral vapor molecules is but 60° while the values in the crystalline forms are near 100°. The P−P separation of 2.21A found in this work is in close agreement with the value 2.20A suggested by Pauling.[20] His As−As value, 2.42A, agrees with the value 2.44 ± 0.03A as found from electron scattering while it is slightly lower than 2.51A from x-ray diffraction.

[20] Linus Pauling, Proc. Nat. Acad. Sci. **18**, 293 (1932).